TABLE III

°C.	Heat of solution, ΔH_S cal./mole
25	202
100	1034
200	2433
300	4163
400	6223
500	8614
600	11335
700	14388

Now

$$RT \ln x + RT \ln \gamma = -T\int_{T_0}^{T} (H^S - H^L)\,(1/T^2)dT \quad (5)$$

γ is the activity coefficient of iron in Hg, T_0 is the melting point of iron (1803°K.), and H^S and H^L are the heat contents of solid and liquid iron, respectively, at the temperature T. Extrapolating Kelley's equations[5] for the heat capacities and heats of transition of the various forms of iron down into the range of these measurements, it follows that approximately

$$4.576T \log_{10} x + 4.576\ T \log_{10} \gamma = -4332 - 21.145T - 3.19 \times 10^{-3}T^2 + 9.256\ T \log_{10} T \quad (6)$$

Combining these equations, the computed activity coefficients of Fe in Hg are given by Table IV.

(5) K. K. Kelley, Contributions to the Data on Theoretical Metallurgy, II, High-Temperature Specific-Heat Equations for Inorganic Substances, U. S. Bureau of Mines Bulletin, 371, 26, Washington, D. C., 1934.

TABLE IV

°C.	γ (activity coefficient of Fe in Hg)	°C.	γ (activity coefficient of Fe in Hg)
50	$0.6 \times 10^{+5}$	400	$2.5 \times 10^{+5}$
100	1.0	450	2.3
150	1.6	500	1.9
200	2.1	550	1.6
250	2.5	600	1.3
300	2.7	650	1.2
350	2.7	700	0.8

It will be noted that the Fe–Hg system shows large positive deviations from Raoult's law, even in extremely dilute solutions. Contrary to the usual behavior of simple systems, the system does not become more uniformly nearly ideal as the temperature is raised, but γ passes through a maximum. This can be explained on the assumption of a negative entropy of mixing amounting to about −24 cal./mole-deg.; *i. e.*, the solution is much less random ("mixed up") than would be expected from simple theory. It is conceivable that this is due to a tendency toward compound formation even in the dilute solutions considered here. Other hypotheses for the nature of the deviations from ideality are also possible.

Summary

The equilibrium solubility of pure iron in pure mercury was determined over the temperature range 25 to 700° C., and an equation developed to express the results.

SCHENECTADY, N. Y. RECEIVED DECEMBER 27, 1949

[CONTRIBUTION FROM THE DEPARTMENT OF CHEMISTRY, COLUMBIA UNIVERSITY]

Particle Size Distribution in Sulfur Hydrosols by Polarimetric Analysis of Scattered Light

BY MILTON KERKER[1] AND VICTOR K. LA MER

The particle size of monodispersed sulfur hydrosols has been determined in this Laboratory by light scattering methods based upon the angular positions of the higher order Tyndall spectra,[1,2,3] the polarization ratio of the scattered light[4] and the optical transmission.[5,6] The results are consistent with the theory of scattering by homogeneous spheres developed by G. Mie.[7]

This paper will (a) extend the polarization ratio method to a range of larger sizes, (b) present a fourth method of size determination, namely, that of phase angle, (c) analyze the size distribution of mixtures of sols and (d) determine the degree of monodispersity of the sulfur hydrosols prepared in this Laboratory.

(1) Clarkson College of Technology, Potsdam, N. Y.
(2) Johnson and La Mer, THIS JOURNAL, **69**, 1184 (1947).
(3) (a) Kenyon and La Mer, *J. Coll. Sci.*, **4**, 163 (1949); (b) Barnes, Kenyon, Zaiser and La Mer, *ibid.*, **2**, 349 (1947).
(4) Sinclair and La Mer, *Chem. Revs.*, **44**, 245 (1949).
(5) Barnes and La Mer, *J. Coll. Sci.*, **1**, 79 (1946).
(6) La Mer and Barnes, *ibid.*, **1**, 71 (1946).
(7) G. Mie, *Ann. Physik*, **25**, 377 (1908).

I. Experimental

A schematic diagram of the light scattering apparatus constructed is shown in Fig. 1. The collimated beam from a high pressure mercury vapor lamp is rendered monochromatic by Corning glass filters. The beam is linearly polarized by a Glan–Thompson prism which can be rotated 180° and whose azimuth can be read to the nearest tenth of a degree.

The scattering cell is cylindrical (75 mm. diameter) except for a small plane window through which the incident beam enters. The refraction of the scattered light on leaving the cell is corrected by a cylindrical lens in the observing system. There is a slot for the insertion of a quarter wave plate of quartz in the path of the scattered light. A second Glan–Thompson prism is used

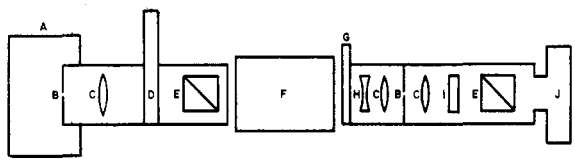

Fig. 1.—Schematic diagram of optical system: A, mercury lamp; B, 1 mm. holes; C, lenses; D, filter; E, Glan–Thompson prism; F, cell; G, shutter; H, cylindrical lens; I, quarter wave plate; J, photomultiplier tube.

as the analyzer. The detector is a 1-P-21 RCA photomultiplier tube. The power supply for this tube is provided by a bank of dry cell batteries (Fig. 2). The output of the photomultiplier tube is sufficient to actuate a sensitive Leeds and Northrup galvanometer provided with a universal shunt. At room temperature and with amplification of 100 volts per stage, the dark current is small and the noise negligible.

PHOTOMULTIPLIER TUBE CIRCUIT

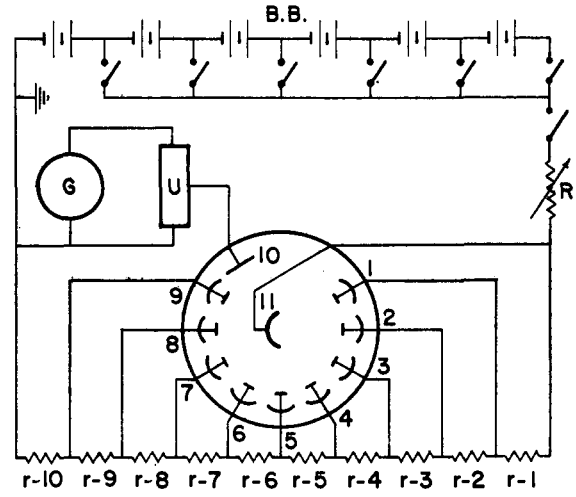

1-9	Dynodes	R	1 Megohm
10	Anode	U	Universal Shunt
11	Photocathode	G	Galvanometer
r-1 – r-10	75,000 Ohms	B.B.	Battery Bank

Fig. 2.

The apparatus is mounted on the stage of a spectroscope. The viewing arm is capable of rotation from 180 to 70° with respect to the incident beam. The angle can be read to the nearest minute. The principal source of error is in the output of the mercury vapor lamp which exhibits erratic fluctuations of about 1% of the output.

The sulfur sols were prepared according to Johnson and LaMer.[1] The relative refractive index of the sulfur particles has been redetermined to be 1.55 for light of wave length 5460 Å. by Mr. Robert Smellie of this Laboratory (private communication). All computations will be for this value.

II. Polarization Ratio Method

Measurements of the polarization ratio, ρ, the ratio of the intensities of the horizontal to vertical components of the scattered light have been used to determine the particle radius[4] provided $\alpha = 2\pi r/\lambda' < 2$ where r is the particle radius and λ' is the wave length relative to the medium. For larger values of α, ρ is no longer monotonic but undergoes highly irregular fluctuations as a function of α.

However, if ρ is plotted as a function of angle of observation for a given value of α, the curve exhibits maxima and minima (Fig. 3) similar to the behavior of the radiation pattern. The angular position and number of these maxima and minima vary in a regular manner with increasing α. For $\alpha > 1.5$, the maxima and minima move toward the forward direction as α increases. New maxima and minima of the polarization ratio continue to arise in the backward direction and move forward as the size increases. The distance between successive maxima and minima continues to decrease so that the number of extrema increases with increasing particle size. The magnitude of the peaks decreases toward the forward direction and the most forward extrema eventually become

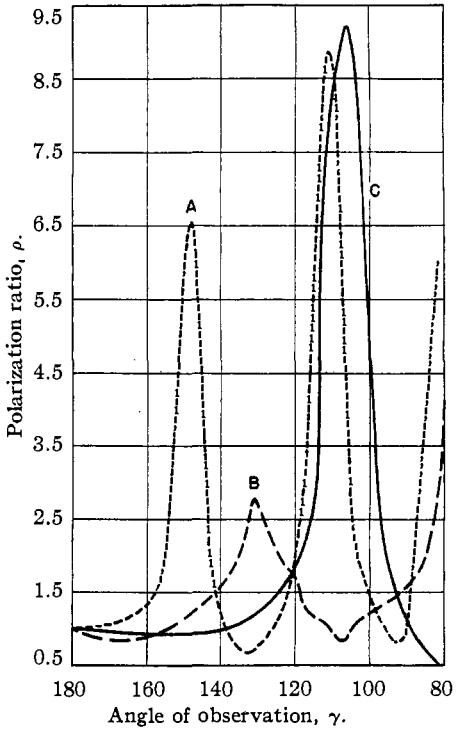

Fig. 3.—Variation of polarization ratio with angle of observation (theoretical, $m = 1.55$): A, $\alpha = 5.0$; B, $\alpha = 4.0$; C, $\alpha = 3.0$.

annulled before reaching the forward direction. The angular positions of these extrema will give a new measure of particle size.

The polarization ratio was measured as a function of angle for a number of sols between $\alpha = 4.5$ and $\alpha = 10.5$. The incident light was unpolarized and of wave length 4360 Å. By using light of wave length 5460 Å., the range was extended to $\alpha = 3.5$.

The particle radii were determined from the time of growth of the sol. The radii were cross-checked on several runs by the transmission method on an aliquot at the same time the polarization ratio measurements were being made. The growth curve obtained previously[1] was reproduced (Fig. 4). The kinetics of this growth has been treated in detail by Zaiser and La Mer.[8]

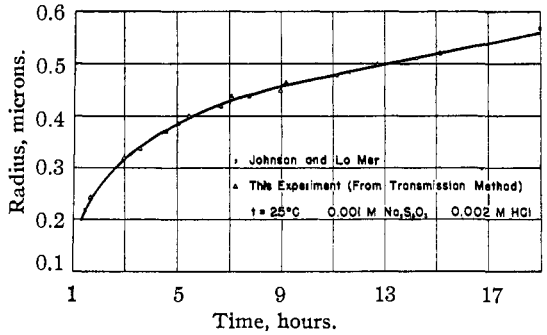

Fig. 4.—Rate of growth of particles.

Some typical curves of polarization ratio *versus* angle of observation are shown in Fig. 5. As predicted by theory, the maxima and minima are pronounced. The values of the polarization ratio are not exactly those predicted by theory, the experimental curves being smoother. This is to be expected since the colloid is not precisely monodispersed. Information as to the extent of polydispersity of the sol will be obtained from this lack of agreement.

The first step in utilizing the polarization ratio curves consists in numbering the maxima and minima. The first maximum and minimum fade out above $\alpha = 6$, so that the first ones observed in the forward direction between $\alpha = 6$ and $\alpha = 9$ should actually be labeled as the second. The angular positions of the maxima and minima as a function of α are presented in Table I. The data are plotted in Fig. 6.

These curves can now be used to determine the particle size of an unknown sol by locating the angular positions of the maxima and minima of the polarization ratio for the unknown on the appropriate curves. An ambiguity in the numbering system can be easily resolved. Thus if the numbering system is wrong, the abscissas plotted on Fig. 6 will not fall on a vertical line and it becomes necessary to adjust the numbering in an appropriate manner (*i. e.*, the first observed maximum may actually belong to the curve for the second or third, etc.).

(8) Zaiser and La Mer, *J. Coll. Sci.*, **3**, 571 (1948).

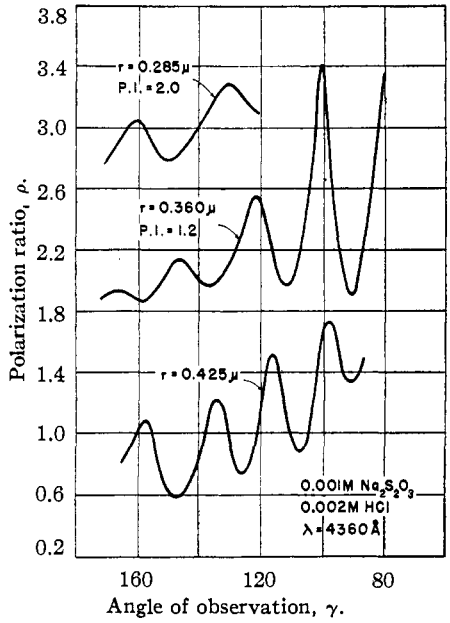

Fig. 5.—Variation of polarization ratio with angle of observation (experimental).

Some theoretical points based upon the Mie theory and Lowan's[9] computations were determined from curves of the type of Fig. 3 and are plotted in Fig. 6. They are in excellent agreement with the experimental results.

In order to obtain the curves of Fig. 3, it was necessary to use interpolated values of the scattering functions for angles intermediate between those available in the Lowan tables. Van de Hulst's[10] interpolation method which involves plotting the amplitude functions in the complex plane was used.

III. Phase Angle Method

If the incident light is linearly polarized, the scattered light will be elliptically polarized. The amplitudes of the horizontal and vertical components of the scattered light are proportional to the amplitudes of the corresponding incident components and are therefore dependent on the azimuth of the incident light. However, the phase difference in amplitudes of the components of the scattered light expressed as phase angle, ϕ, is independent of the orientation of the incident light and a function only of the index of refraction of the particle and α. It is possible, therefore, to use the phase angle as a measure of particle size.

To calculate the phase angle, it is necessary to utilize the complex functions i_1^* and i_2^*. They are related to a, the intensity of the vertical com-

(9) Lowan, "Tables of Scattering Functions for Spherical Particles," National Bureau of Standards, Applied Mathematics Series—4.

(10) Van de Hulst, *J. Coll. Sci.*, **4**, 79 (1949).

TABLE I

ANGULAR POSITIONS OF MAXIMA AND MINIMA OF POLARIZATION RATIO AS A FUNCTION OF PARTICLE RADIUS

Radius, mμ	α	1st Max.	1st Min.	2nd Max.	2nd Min.	3rd Max.	3rd Min.	4th Max.	4th Min.	Radius, mμ	α	2nd Max.	2nd Min.	3rd Max.	3rd Min.	4th Max.	4th Min.	5th Max.	5th Min.	6th Max.	6th Min.
232[a]	3.50	124	...	...	...	...	...	...	..	378	7.26	152	141	127	118	108	100	...	...	...	...
262[a]	3.95	131	109	...	...	...	...	...	..	390	7.50	153	142	129	119	110	99	89	...	...	...
275[a]	4.14	134	115	...	...	...	...	...	..	402	7.73	154	144	130	119	111	101	93	...	...	...
296[a]	4.47	140	120	102	...	...	...	...	..	417	8.02	157	146	134	124	115	106	97	88	80	...
249	4.78	142	...	...	...	...	...	...	..	436	8.37	160	149	138	129	119	110	101	93	84	...
258	4.97	149	132	...	...	...	...	...	..	448	8.62	162	151	141	131	122	113	105	97	87	...
269	5.17	154	141	121	...	...	...	...	..	458	8.81	163	153	144	134	124	118	107	100	88	83
282	5.42	160	150	130	...	...	...	...	..	472	9.06	165	158	148	138	129	120	112	104	95	87
309	5.93	166	157	134	119	105	91	...	..	508	9.77	...	165	153	145	137	128	122	115	107	97
325	6.24	167	159	140	127	114	103	91	..	522	10.03	...	...	157	151	142	133	125	119	113	106
350	6.72	...	...	145	136	121	111	100	89	546	10.49	...	...	...	157	152	141	132	127	121	114
364	6.99	...	...	147	137	122	112	102	92	...	...	...	...	...	...	...	...	...	...	...	...

[a] λ = 5460 Å.

ponent, and b, the intensity of the horizontal component of the scattered light by

$$a = \left(\frac{\lambda}{2\pi}\right)^2 i_1 = \left(\frac{\lambda}{2\pi}\right)^2 |i_1^*|^2$$
$$b = \left(\frac{\lambda}{2\pi}\right)^2 i_2 = \left(\frac{\lambda}{2\pi}\right)^2 |i_2^*|^2 \qquad (1)$$

Then

$$\tan\phi = \frac{i_1^* \times i_2^*}{i_1^* \cdot i_2^*} \qquad (2)$$

where the numerator and denominator represent, respectively, the vector and scalar products of the complex functions. The interpolated values of these quantities obtained for the polarization ratio method were used to interpolate additional values of tan ϕ.

The phase angle exhibits a series of sharp maxima and minima both as a function of particle radius and angle of observation. An analysis analogous to that used for the polarization ratio was employed.

To determine tan ϕ, it is necessary to measure the following quantities

i_3, intensity of light scattered with analyzer oriented 45° from the vertical
i_4, intensity of light scattered with analyzer oriented 135° from the vertical
i_5, same as i_3 with quarter wave plate in place
i_6, same as i_4 with quarter wave plate in place

It will be shown later that

$$\tan\phi = \frac{i_5 - i_6}{i_3 - i_4} \qquad (3)$$

Typical experimental curves of tan ϕ against angle of observation are shown in Fig. 7. The

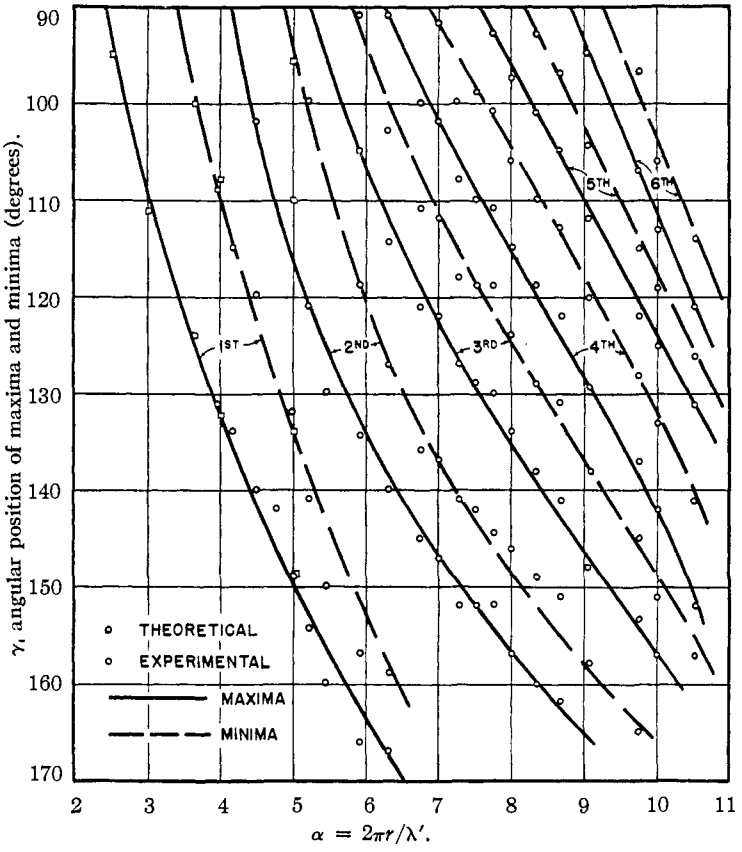

Fig. 6.—Angular positions of maxima and minima of polarization ratio as a function of α.

Tan ϕ was determined for a number of sols between α = 3.5 and α = 8.0. The quarter wave plate produced a retardation of 96° for the 5460 Å. mercury line. A correction formula has been developed to be used when the quarter wave plate has a retardation different from 90°. The error caused by the 6° shift is not significant. The angular positions of the maxima and minima of tan ϕ are shown in Table II. The particle radius was calibrated in terms of the polarization ratio and transmission.

maxima and minima have been treated exactly as for the polarization ratio. The angular positions of the maxima and minima are plotted as a function of α in Fig. 8. The points calculated from the theory coincide with the experimental curves.

IV. Size Distribution of Polydispersed Systems

Although it is not practical to analyze a continuous distribution of sizes by the light scattering technique, it is possible to treat simple mixtures of

TABLE II

ANGULAR POSITIONS OF MAXIMA AND MINIMA OF TANGENT OF PHASE ANGLE AS A FUNCTION OF PARTICLE RADIUS

Radius, microns	α	1st Max.	1st Min.	2nd Max.	2nd Min.	3rd Max.	3rd Min.	4th Max.	4th Min.
0.210	3.22	118							
.232	3.49	133	107						
.261	3.99	143	126						
.275	4.14	141	128	103					
.280	4.29	148	132	108	92				
.294	4.50	152	139	119	104	90			
.308	4.72		148	127	114	101	84		
.338	5.18			136	125	109	98	84	76
.369	5.65			142	132	118	108	95	86
.362	5.55			141	131	118	107	93	84
.388	5.95			147	138	125	114	100	85
.406	6.22			151	142	129	120	103	94
.433	6.63				145	131	122	112	103
.476	7.30				149	138	129	119	110
.535	8.17					147	139	129	120

monodispersed sols. The intensity scattered at the angle of observation, γ, by an n-component mixture is

$$I(\gamma) = \sum_{i=1}^{n} x_i I(\gamma, r_i) \qquad (4)$$

where x_1 is the fractional concentration of component i and $I(\gamma, r_i)$ is the intensity scattered by component i. It is necessary to make observations at only $n - 1$ different angles because of the additional relation

$$\sum_{i=1}^{n} x_i = 1 \qquad (5)$$

The resulting simultaneous equations may then be solved for the x_i's.

Mixtures containing more than three components could not be analyzed by this method because the successive differencing of the experimental data required in solving the simultaneous equations produces increasingly larger errors as the number of equations to be solved increases.

In practice it was best to take more data than actually necessary to carry out the calculation. Since the principal error arises from the small differences between the experimental quantities, it was possible to choose by inspection that set of data most likely to give precise results.

The results for two and three component systems are presented in Table III. The values of $I(\gamma, r_1)$ were determined experimentally rather than from the theoretical tables. The scattering measurements were made first on the components and then on the mixture. The procedure was checked by carrying out dilution experiments on several sols (Fig. 9). The scattered intensity was exactly proportional to dilution which justifies the assumption that secondary scattering is negligible.

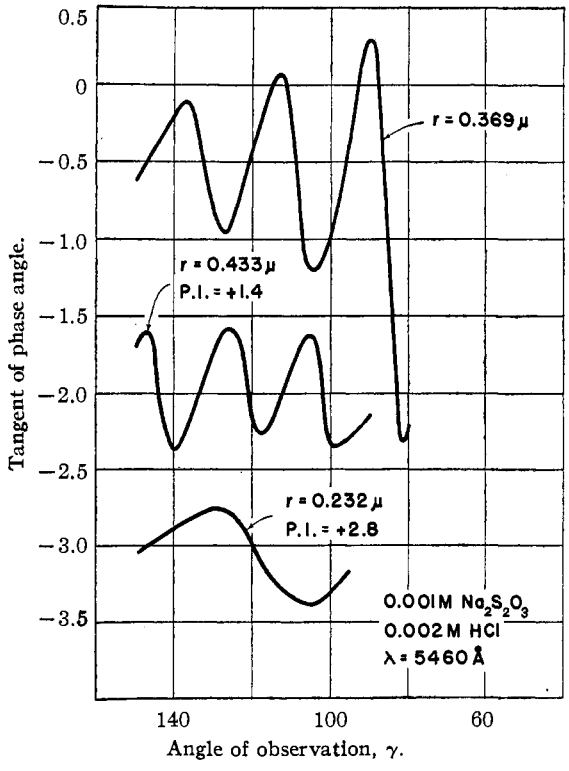

Fig. 7.—Variation of tangent of phase angle with angle of observation (experimental).

TABLE III

ANALYSIS OF MIXTURES OF MONODISPERSED SOLS FROM INTENSITY OF SCATTERED LIGHT

Run	Radii of components, microns	% Composition Calcd.	% Composition Found
M-19	0.26 0.40	50.0 50.0	48.4 51.6
M-20	.26 .42	50.0 50.0	52.9 47.1
M-21	.26 .40	50.0 50.0	50.6 49.4
M-30	.26 .41	50.0 50.0	50.8 49.2
M-26	.26 .41	33.3 66.7	37.9 62.1
M-27	.26 .41	33.3 66.7	33.0 67.0
M-31	.26 .41	33.3 66.7	31.7 68.3
M-33	.26 .39	33.3 66.7	34.9 65.1
M-37	.26 .35 0.58	33.3 33.3 33.3	34.6 31.2 34.2
M-38	.26 .39 .59	33.3 33.3 33.3	30.2 35.8 34.0
M-41	.26 .35 .58	33.3 33.3 33.3	32.1 39.1 28.7
M-39	.26 .33 .54	25.0 50.0 25.0	26.3 49.6 24.1
M-40	.26 .38 .58	25.0 50.0 25.0	27.0 46.4 26.6

An analysis, completely analogous to the above, can be carried out using the optical density of the sols. Thus

$$D(\lambda) = \sum_{i=1}^{n} x_i D(\lambda, r_i) \qquad (6)$$

where $D(\lambda)$ is the optical density of the mixture at wave length λ and $D(\lambda, r_i)$ the optical density of the component of radius r_i at this wave length. The experimental procedure was similar to the above, *i. e.*, the optical densities of the components were determined first and then that of the mixture was obtained. It was necessary to take data at different wave lengths to obtain the requisite number of equations. The results are presented in Table IV.

TABLE IV

ANALYSIS OF MIXTURES OF MONODISPERSED SOLS FROM OPTICAL DENSITY

Run	Radii of components, microns	% Composition Calcd.	% Composition Found
M-1	0.26 0.37	50.0 50.0	51.2 48.8
M-2	.26 .38	50.0 50.0	52.8 47.2
M-3	.26 .40	50.0 50.0	54.7 45.3
M-5	.26 .40	50.0 50.0	47.2 52.8
M-7	.26 .40	50.0 50.0	50.4 49.6
M-12	.26 .41	50.0 50.0	48.5 51.5
M-16b	.26–.42	33.3 66.7	31.8 68.2
M-17a	.26 .45	66.7 33.3	65.1 34.9
M-17b	.26 .45	33.3 66.7	36.4 63.6
M-9	.26 .38 0.43	33.3 33.3 33.3	32.9 34.8 32.3
M-13	.26 .39 .43	33.3 33.3 33.3	35.0 30.4 34.6
M-14	.26 .41 .45	33.3 33.3 33.3	35.3 30.1 34.5
M-10	.26 .40 .43	50.0 25.0 25.0	51.6 27.7 20.7
M-11	.26 .43 .48	50.0 25.0 25.0	60.1 23.7 16.3
M-15	.26 .40 .48	25.0 50.0 25.0	23.9 50.3 25.8

V. Size Distribution of Monodispersed Sulfur Sols

A truly monodispersed colloid is a mathematical limit which can never be attained in nature. The sulfur sols prepared in this Laboratory are certainly more monodispersed than any others that have been reported because of the brilliance of the higher order Tyndall spectra which they exhibit. Nevertheless, it is desirable to have a more quantitative criterion of monodispersity so that the extent of size distribution tolerated by sols exhibiting higher order Tyndall spectra can be ascertained.

To simplify calculations, the type of distribution to be considered will be a uniform distribution, *i. e.*, one for which the distribution function is constant within the specified limits and equal to zero outside these limits.

The effect of such a distribution on the sharpness of the orders in the Tyndall spectra will be considered first. In Fig. 10 curves are plotted for the ratio of red to green scattered light as a function of angle between $\gamma = 110°$ and $\gamma = 160°$ for four size distributions. It is apparent that the sharpness of the orders decreases as the polydispersity increases. Eventually a situation is reached where the orders are obliterated.

However, the existence of orders (*i. e.*, a red to green ratio differing sensibly from one) is not a sufficient criterion for absolute monodispersity as can be seen by examining the curve for distribution B. The outside limits of this distribution differ by 10% from the value of the median and yet such a distribution would exhibit a red order at 125° for which the ratio of red to green scattered light is 4.3.

To determine the extent of the size distribution for one of these relatively monodispersed sols, it would be necessary to compare the experimental curve with a family of theoretical curves such as those in Fig. 10. Such an analysis can be carried out with polarization ratio data as well as the order patterns. In Fig. 11, curve C represents the experimental values of the polarization ratio of a sol corresponding to $\alpha = 3.5$ and plotted on the same graph are the polarization ratio curves calculated for several uniform size distributions having as their median, $\alpha = 3.5$. The polarization ratio of the distributions is obtained by integrating graphically the intensity functions for the horizontal and vertical components of the scattered light and taking the appropriate ratios of the integrated quantities.

It can be seen that just as for the case of the orders, the effect of polydispersity is to decrease the sharpness of the maxima and minima in the curves and ultimately to distort the pattern of the monodispersed sol. By comparison of the experimental curve with the theoretical curves, it appears that this sol can be represented by one of

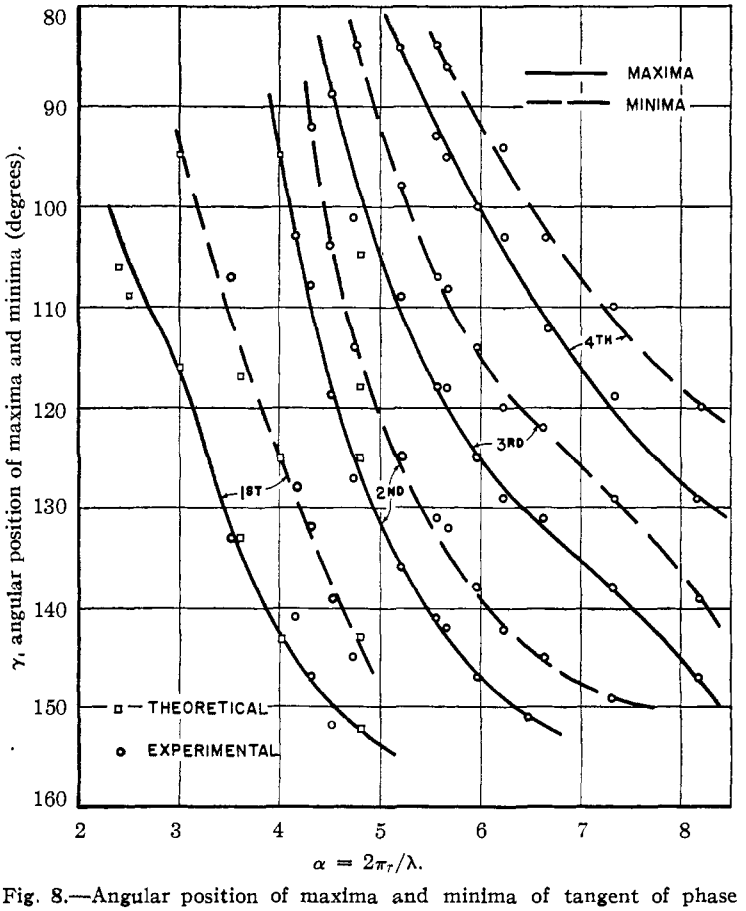

Fig. 8.—Angular position of maxima and minima of tangent of phase angle as function of α.

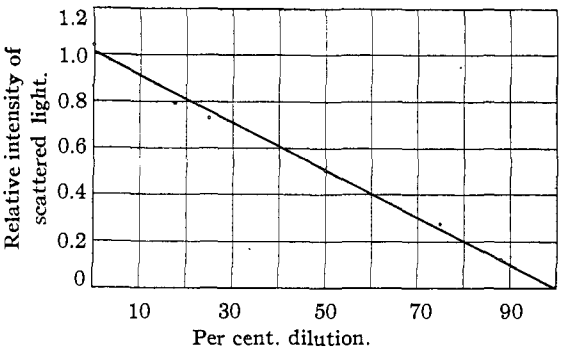

Fig. 9.—Effect of dilution on scattered intensity.

uniform distribution with outer limits differing from the median by about 10%. Examination of several sols in this manner indicates that the sulfur sols prepared according to the methods used in this Laboratory have scattering properties similar to those calculated for sols with uniform distributions with outer limits differing from the median by 5 to 10%. To estimate the shape of the distribution curve, more accurate data and more extensive theoretical computations would be required than are available at present.

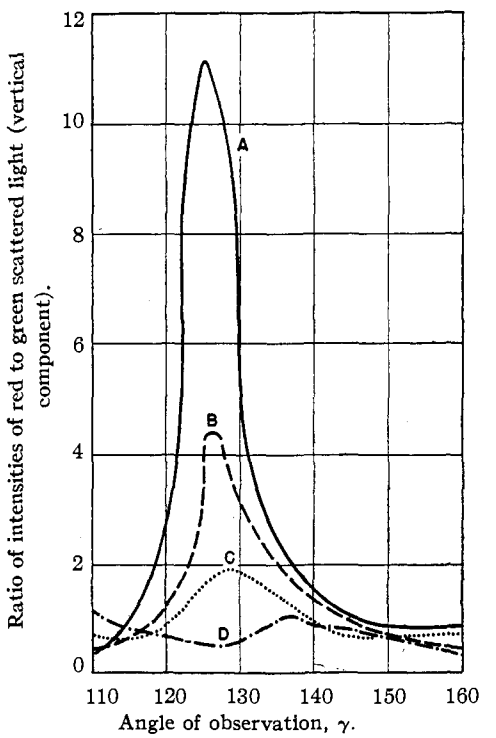

Fig. 10.—Effect of size distribution on orders calculated from Mie theory: red light, 6600 Å.; green light, 5500 Å.: A, r 0.24 micron (monodispersed); B, r 0.216–0.252 micron*; C, r 0.180–0.300 micron*; D, r 0.120–0.360 micron*. * = uniform distributions.

VI. Criterion for Monodispersity

Since the existence of higher order Tyndall spectra is not sufficient proof of absolute monodispersity, a more sensitive and quantitative criterion of monodispersity is desirable. Soleillet,[11] F. Perrin[12] and H. Mueller[13] have given a criterion that serves our purpose.

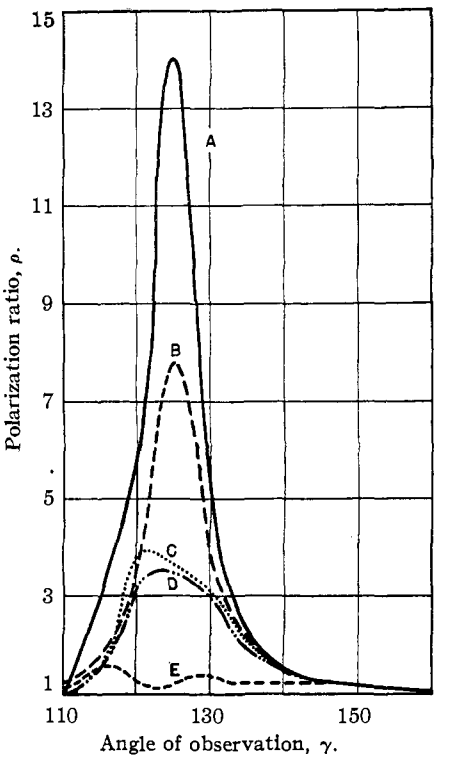

Fig. 11.—Effect of size distribution on polarization ratio calculated from Mie theory: A, α = 3.50 (monodispersed); B, α = 3.30–3.70*; C, α = 3.50 (experimental); D, α = 3.15–3.85*; E, α = 2.80–4.20*. * = Uniform distribution.

As shown above, if the incident light is linearly polarized, the scattered light will be elliptically polarized. Each particle size will scatter a characteristic type of such elliptically polarized light so that if there are particles of more than one size, it will be necessary to superpose incoherently light of different ellipticities. The resultant of such a process will be light which consists of two parts, one which is natural light and the other elliptically polarized light.

The quantitative criterion for monodispersity can now be stated. If, for linearly polarized incident light, the scattered light is completely elliptically polarized, the sol is monodispersed. If the scattered light is partially elliptically polarized the sol is polydispersed.

To determine the exact character of the scattered light for a mixture of monodispersed sols or for a polydispersed sol, it becomes necessary to superpose the characteristic vibration ellipses of the different particle sizes. This is normally a tedious process unless the parameters describing

(11) Soleillet, *Ann. Phys.*, **12**, 23 (1929).
(12) F. Perrin, *J. Chem. Phys.*, **10**, 415 (1942).
(13) H. Mueller, private communication.

the vibration ellipses are defined in a manner specified by Stokes.[14]

A completely polarized monochromatic beam of light can be described by two orthogonal electric vectors having a fixed phase difference ϕ. In general, the resultant vector will sweep out an ellipse, hence the name, elliptically polarized light. If the amplitudes of the vectors are p_1 and p_2, the Stokes parameters are defined by

$$\begin{aligned} I &= p_1^2 + p_2^2 \\ M &= p_1^2 - p_2^2 \\ C &= 2p_1p_2 \cos \phi \\ S &= 2p_1p_2 \sin \phi \end{aligned} \tag{7}$$

The value of the Stokes parameters lies in the fact that for the incoherent superposition of light from different sources, the Stokes parameters are additive. Thus if the characteristic vibration ellipses for the scattered light of each particle size can be expressed in terms of Stokes parameters, it becomes a simple matter to calculate the state of polarization of the light scattered by any mixture or distribution of sizes.

Furthermore, it can be shown that for completely polarized light, the equality below is valid, while for partially polarized light, the inequality subsists.

$$P \equiv \left(\frac{M}{I}\right)^2 + \left(\frac{C}{I}\right)^2 + \left(\frac{S}{I}\right)^2 \leq 1 \tag{8}$$

The quantity P will be called the monodispersity factor. For a monodispersed system, $P = 1$, while for a polydispersed system $P < 1$.

The Stokes parameters of the scattered light can be expressed in terms of the results of the Mie theory

$$\begin{aligned} I &= \left(\frac{\lambda}{2\pi}\right)^2 (i_1 \cos^2 \psi + i_2 \sin^2 \psi) \\ M &= \left(\frac{\lambda}{2\pi}\right)^2 (i_1 \cos^2 \psi - i_2 \sin^2 \psi) \\ C &= \left(\frac{\lambda}{2\pi}\right)^2 i_1^* \cdot i_2^* \sin 2\psi \\ S &= \left(\frac{\lambda}{2\pi}\right)^2 i_1^* \times i_2^* \sin 2\psi \end{aligned} \tag{9}$$

where ψ gives the orientation of the incident vector with respect to the vertical direction.

If I_r, M_r, C_r and S_r are the Stokes parameters calculated for particles of radius r and if $P(r)\,dr$ is the distribution function, then the Stokes parameters for the light scattered by a polydispersed sol are given by

$$\begin{aligned} I &= \int_0^\infty I_r P(r) dr \\ M &= \int_0^\infty M_r P(r) dr \\ C &= \int_0^\infty C_r P(r) dr \\ S &= \int_0^\infty S_r P(r) dr \end{aligned} \tag{10}$$

In the case of a mixture of monodispersed systems, the integration would be replaced by a summation.

Soleillet[11] has proposed that the Stokes parameters be determined in the following manner. Let the scattered light be observed through a double image prism such as a Wollaston or Rochon prism. Then with the double image prism oriented with one of its axes in the vertical direction, the orientation of the analyzer with respect to the vertical direction when the analyzer brings the two fields in the double image prism to equal intensity will be called α_1. If the double image prism is rotated 45°, the matching position of the analyzer with respect to the direction 45° from the vertical will be called α_2. If now a quarter wave plate be inserted between the double image prism and the scattering medium, the corresponding position of the analyzer will be called α_3. Then it can be shown that

$$\begin{aligned} \tan^2 \alpha_1 &= \frac{I - M}{I + M} & \cos 2\alpha_1 &= \frac{M}{I} \\ \tan^2 \alpha_2 &= \frac{I - C}{I + C} & \cos 2\alpha_2 &= \frac{C}{I} \\ \tan^2 \alpha_3 &= \frac{I - S}{I + S} & \cos 2\alpha_3 &= \frac{S}{I} \end{aligned} \tag{11}$$

We now extend Soleillet's proposal as follows. It is well known that $\tan^2 \alpha$ as determined above gives the ratio of the intensities of the two orthogonal components of the light, the azimuths of the components being determined by the azimuth from which α is determined. It then follows that

$$\begin{aligned} \tan^2 \alpha_1 &= a/b & \cos^2 \alpha_1 &= \frac{a - b}{a + b} \\ \tan^2 \alpha_2 &= i_3/i_4 & \cos 2\alpha_2 &= \frac{i_3 - i_4}{i_3 + i_4} \\ \tan^2 \alpha_3 &= i_5/i_6 & \cos 2\alpha_3 &= \frac{i_5 - i_6}{i_5 + i_6} \end{aligned} \tag{12}$$

where a and b are the intensities of the vertical and horizontal components of the scattered light and i_3, i_4, i_5 and i_6 are defined above equation 3. All six of these quantities can be measured with the apparatus described previously. Furthermore

$$I = a + b = i_3 + i_4 = i_5 + i_6 \tag{13}$$

It follows from (11), (12) and (13) that

$$\begin{aligned} M &= a - b \\ C &= i_3 - i_4 \\ S &= i_5 - i_6 \end{aligned} \tag{14}$$

The verification of equation (3) is now obvious since

$$\tan \phi = \frac{S}{C} = \frac{i_5 - i_6}{i_3 - i_4} \tag{15}$$

Our formulation (14) shows clearly why the Stokes parameters have the remarkable property of being additive. It is because they can be expressed as a linear combination of intensity functions. It is shown in textbooks of physical optics[15] that a property of the light intensity is its

(14) G. G. Stokes, *Trans. Camb. Phil. Soc.*, **9**, 3999 (1852).

(15) Jenkins and White, "Fundamentals of Physical Optics," McGraw-Hill Book Co., Inc., New York, N. Y., 1937.

additivity in the superposition of incoherent beams.

The monodispersity factors measured for three typical sols at three angles of observation are given in Table V. These values have been normalized to correspond to an incident polarized beam whose azimuth is at 45° so that the experimental results can be compared to the theoretical data computed for horizontal and vertical components of equal intensity (*i. e.*, when these components are in phase, the light is linearly polarized at 45°).

TABLE V

MONDISPERSITY FACTOR P AS A FUNCTION OF SIZE DISTRIBUTION

The theoretical values of P have been computed for uniform distributions D-1, D-2, D-3, D-4, D-5 for which the mean of the distribution equals the value of α in the 2nd column and the outer limits differ from the mean by 2, 5, 10, 20 and 50%, respectively

			Monodispersity factor, P					
Run	α	Angle γ	Experimental	D-1	D-2	D-3	D-5	D-5
F-34	4.6	110	0.65	0.83	0.64	0.69	0.51	
		130	.88	0.93	.94	.82	.53	
		150	.99	1.00	.94	.93	.83	
F-35	3.0	110	.69	1.00	.93	.91	.69	0.55
		130	.87	0.95	.85	.78	.64	.63
		150	.98	.97	.98	.99	.97	.95
F-37	4.2	110	.84	.96	.88	.60	.51	
		130	.78	.94	.92	.86	.72	
		150	.92	1.00	.96	.94	.89	

Theoretical values of the monodispersity factor, P, are presented for uniform distributions, the median of the distribution in each case equaling the value of α of the sol in question. It should be possible therefore to obtain some information about the extent of the size distribution in each sol by comparing its monodispersity factor with those of the theoretical distributions.

The Stokes parameters for the distributions were obtained from curves of Stokes parameters *versus* α by graphical integration. Again the Lowan tables proved insufficient so that it was necessary to use some interpolated values of the Stokes parameters. The monodispersity factor was calculated by equation (8).

The monodispersity factor behaves in an even more irregular manner than any of the other functions heretofore described. The Stokes parameters represent differences of intensity functions which themselves have been shown to be irregular functions of the experimental variables. The monodispersity factor is calculated by squaring these differences so that the lack of regularity is not difficult to account for.

One regular feature about P is its tendency to approach a value of 1 in the forward scattering directions. Thus for the three sols tabulated P values at 110° were 0.69, 0.84 and 0.65 while at 150° these same sols exhibited values of P equal to 0.98, 0.92 and 0.99. This is in agreement with the values calculated theoretically which show furthermore that the monodispersity factor decreases more slowly from 1 with increasing polydispersity at the more forward directions.

The two components of the light are scattered in the forward direction with equal intensity but with a phase difference of 180°. Therefore if the incident light is linearly polarized, the scattered light will be linearly polarized but its azimuth will have changed. If the sol is polydispersed, the light will be linearly polarized light since each size will scatter the same kind of linearly polarized light in the forward direction. The monodispersity factor will accordingly always be unity in the forward direction. Therefore P will be a much more sensitive criterion of monodispersity if observed at the transverse rather than the forward direction.

From the magnitudes of the observed values of P, it appears that our sols involve distributions with outside limits differing from the median by 5 to 20%. However, the method described previously which utilized the polarization ratio gave more precise information about the size distribution than does P. Indeed, the polarization data are included in the monodispersity factor but the complicated treatment of the data used in calculating P makes the interpretation of the latter more difficult.

It is true, however, that with increasing polydispersity, the value of P decreases toward zero no matter how erratic its path. Thus a very dense sol of gum arabic for which the secondary scattering also was pronounced and which was probably highly polydispersed gave $P = 0.01$. The monodispersity factor is most useful for setting up a criterion of absolute monodispersity and may be used to give a rough estimate of the deviations from monodispersity.

Acknowledgment.—The authors are indebted to Professor Hans Mueller of Massachsetts Institute of Technology for two stimulating conferences and a lucid unpublished exposition of the theory of light scattering involved in this work. He suggested that we investigate the Stokes parameters of the light scattered from our sols and to apply the Mie theory for calculations. It was due to a remark in his unpublished communication that the phase angle method was developed.

Summary and Conclusions

A photoelectric light scattering apparatus has been constructed which is capable of analyzing scattered light including elliptically polarized light as a function of angle of observation. The incident light may be natural or linearly polarized in any desired azimuth.

Two new methods of determining particle size in the size range where the wave length is comparable to the particle radius have been developed. They depend upon observing the polarization ratio and phase angle as a function of angle of ob-

servation. The angular positions of the maxima and minima of these quantities can be used to determine the particle radius. These methods extend the number of optical methods now available to four, the others being the spectral orders and transmission methods.

The determination of the concentrations of the components of a mixture of three monodispersed sols are amenable to practical treatment.

The effect of polydispersity on the higher order Tyndall spectra has been discussed and theoretical calculations have been made to show the effect of increasing the size distribution. An analysis utilizing the polarization ratio data indicates that the scattering properties of the sulfur sols prepared according to the methods developed in this Laboratory are similar to those with uniform distributions whose limits differ from the median by 5 to 10%.

Stokes parameters have been utilized to set up a criterion for monodispersity. A monodispersity factor P has been defined which will have the value 1 for an absolutely monodispersed system and a value less than 1 for a polydispersed system. Measures of monodispersity factors have been presented for several sols. The values of P are less than 1 but the range of values indicates that the sols are within the size distribution limits determined by the polarization ratio method. The latter method is superior for determination of the extent of size distribution although the monodispersity factor is a valuable and useful criterion of absolute monodispersity.

NEW YORK 27, N. Y. RECEIVED OCTOBER 8, 1949

[CONTRIBUTION FROM THE RESEARCH AND DEVELOPMENT LABORATORIES, UNIVERSAL OIL PRODUCTS COMPANY]

The Peroxide-Induced Exchange of Hydrogen and Chlorine between Saturated Hydrocarbons and Polychloroalkanes[1]

BY JAMES P. WEST AND LOUIS SCHMERLING

When a saturated hydrocarbon is treated with certain polyhalogenated hydrocarbons in the presence of a catalytic amount of a decomposing organic peroxide, hydrogen–halogen exchange occurs and the hydrocarbon is converted to a monohaloalkane. Thus, for example, the reaction of isobutane with carbon tetrachloride in the presence of di-*t*-butyl peroxide at 130–140° results in the formation of *t*-butyl chloride and chloroform. The reaction presumably is a chain reaction

$$R'OOR' \longrightarrow 2R'O\cdot \text{ (e. g., R' = } t\text{-}C_4H_9 \text{ or } C_6H_5CO) \quad (1)$$

$$R'O\cdot + RH \longrightarrow R\cdot + R'OH \quad (2)$$

$$R\cdot + CCl_4 \longrightarrow RCl + Cl_3C\cdot \quad (3)$$

$$Cl_3C\cdot + RH \longrightarrow Cl_3CH + R\cdot \quad (4)$$

The alkyl radical formed as in step 4 begins a new cycle as in step 3. Chain-terminating reactions involve the interaction of the alkyl and/or trichloromethyl radicals; crystalline hexachloroethane was isolated as a minor by-product in many of the reactions studied.

The result with isobutane is of particular interest in view of the observation[2] that the *t*-butyl radical formed by decomposing bis-trimethylacetyl peroxide (unlike the methyl, *n*-propyl and isopropyl radicals formed from diacetyl, di-*n*-butyryl and diisobutyryl peroxide, respectively) is of insufficient activity to abstract a chlorine atom from carbon tetrachloride. It may be significant that the experiment with the diacyl peroxide was carried out in "warm carbon tetrachloride" while that with isobutane was run at 130–140°.[3]

Experiments with a variety of saturated hydrocarbons and polychloromethanes and -ethanes are summarized in Tables I and II. Good yields of heptyl chlorides, principally a mixture of *s*-heptyl chlorides, were obtained by the conversion of *n*-heptane. Even propane was found to react, a rather good yield of isopropyl chloride being obtained by the reaction of propane with carbon tetrachloride in the presence of di-*t*-butyl peroxide at 138°. On the other hand, no hydrogen–chlorine exchange reaction occurred when ethane was used under similar conditions.

In general, chlorination occurred preferentially at tertiary carbon atoms, probably because of the relative ease of abstraction of a hydrogen atom from a tertiary carbon atom. With bicyclo[2.2.1]heptane, however, the major product was the secondary chloride, 2-chlorobicyclo[2.2.1]heptane, rather than the bridgehead tertiary chloride, 1-chlorobicyclo[2.2.1]heptane, which may also have been formed.

When hexachloroethane is used as the halogen donor, alkyl chloride is obtained in excellent yield, but the other anticipated product, the pentachloroethane, is not formed. Instead, tetra-

(1) Presented before the Division of Organic Chemistry at the 116th Meeting of the American Chemical Society, Atlantic City, September, 1949.

(2) A. B. Ash and H. C. Brown, *Record Chem. Progress* (*Kresge-Hooker Sci. Lib.*, **9**, 90 (1948); *cf.* M. S. Kharasch, S. S. Kane and H. C. Brown, THIS JOURNAL, **64**, 1622 (1942).

(3) NOTE ADDED IN PROOF.—On the other hand, the difference in results may be taken as an indication that the acyl peroxide decomposes to yield trimethylacetate radicals rather than *t*-butyl radicals and carbon dioxide; *cf.* F. G. Edwards and F. R. Mayo, *ibid.*, **72**, 1268 (1950).